

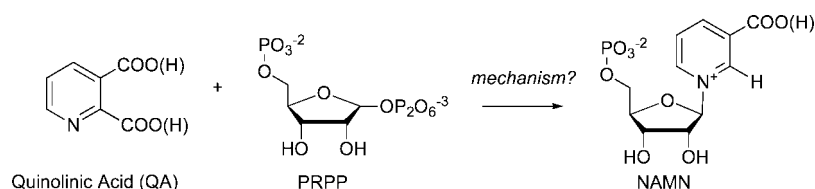
Theoretical Studies of the Quinolinic Acid to Nicotinic Acid Mononucleotide Transformation

Aleksandr Rozenberg and Jeehiun K. Lee*

Department of Chemistry and Chemical Biology, Rutgers, The State University of New Jersey, Piscataway, New Jersey 08854

jeehiun@rci.rutgers.edu

Received June 09, 2008



Quinolinic acid phosphoribosyl transferase (QPRTase) is an essential enzyme that catalyzes the transformation of quinolinic acid (QA) to nicotinic acid mononucleotide (NAMN), a key step on the *de novo* pathway for nicotinamide adenine dinucleotide (NAD) biosynthesis. We describe herein a theoretical study of the intrinsic energetics associated with the possible mechanistic pathways by which QA forms NAMN. Our main interest is in probing the decarboxylation step, which is intriguing since the product is a vinylic anion, not unlike the reaction catalyzed by orotidine 5'-monophosphate (OMP) decarboxylase, an enzyme whose mechanism is under fierce debate. Our calculations indicate that a path involving a quinolinic acid mononucleotide (QAMN) intermediate is the most energetically attractive, favoring decarboxylation. We also find that the monocarboxylate form of QAMN will decarboxylate much more favorably energetically than will the dicarboxylate form of QAMN. Furthermore, our calculations indicate that decarboxylation is not a likely first step; the substrate in such a mechanism would prefer to decarboxylate at the C3 position, not the desired C2 position. We also discuss our results in the context of existing experimental data.

Introduction

In both prokaryotes and eukaryotes, quinolinic acid phosphoribosyl transferase (QPRTase), a type II PRTase, is an essential enzyme that lies on the *de novo* pathway for nicotinamide adenine dinucleotide (NAD) biosynthesis.^{1–8} The enzyme is specific in catalyzing the reaction of quinolinic acid (QA) and 5'-phosphoribosyl-1'-pyrophosphate (PRPP) in the presence of

a magnesium cation to form pyrophosphate, carbon dioxide, and nicotinic acid mononucleotide (NAMN, Scheme 1).^{9–12}

QPRTase is a target for several health and agricultural applications. *Mycobacterium tuberculosis* (MTB)—the lethal pathogen causing tuberculosis—relies on the *de novo* pathway for NAD biosynthesis.¹³ Because humans have two pathways for NAD generation (salvage in addition to the *de novo* route), inhibition of QPRTase (and therefore the *de novo* NAD synthesis pathway) is an attractive option for tuberculosis therapy.^{13–17} Quinolinic acid is also a potent excitotoxin in human brain tissue, and a correlation is found between neuro-inflammatory disease and an increased concentration of quino-

(1) Begley, T. P.; Kinsland, C.; Taylor, S.; Tandon, M.; Nicewonger, R.; Wu, M.; Chiu, H.-J.; Kelleher, H.; Campobasso, N.; Zhang, Y. In *Biosynthesis: Polyketides and Vitamins*; Leeper, F. J., Vederas, J. C., Eds.; Springer-Verlag: New York, 1998; Vol. 195, pp 93–142.

(2) Bhatia, R.; Calvo, K. C. *Arch. Biochem. Biophys.* **1996**, *325*, 270–278, and references therein.

(3) Cao, H.; Pietrak, B. L.; Grubmeyer, C. *Biochemistry* **2002**, *41*, 3520–3528.

(4) Nagano, N.; Orengo, C.; Thornton, J. M. *J. Mol. Biol.* **2002**, *321*, 741–765.

(5) Rizzi, M.; Schindelin, H. *Curr. Opin. Struct. Biol.* **2002**, *12*, 709–720.

(6) White, H. B. In *Pyridine Coenzyme Nucleotides*; Everse, J., Anderson, B., You, K. S., Eds.; Academic Press: New York, 1982; pp 1–17.

(7) Gaur, R.; Roberts, T.; Calvo, K. *Protein Pept. Lett.* **2006**, *13*, 163–167.

(8) Packman, P. M.; Jakoby, W. B. *J. Biol. Chem.* **1967**, *242*, 2075–2079.

(9) Gholson, R.; Ueda, I.; Ogaswara, N. *J. Biol. Chem.* **1964**, *239*, 1208–1214.

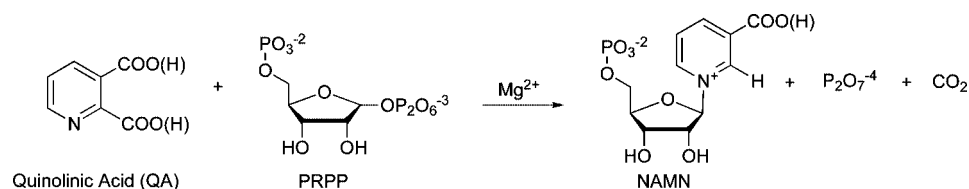
(10) Kalikin, L.; Calvo, K. C. *Biochem. Biophys. Res. Commun.* **1988**, *152*, 559–564.

(11) Mattevi, A. *Nat. Struct. Mol. Biol.* **2006**, *13*, 563–564.

(12) Rich, P. R. *Biochem. Soc. Trans.* **2003**, *31*, 1095–1105.

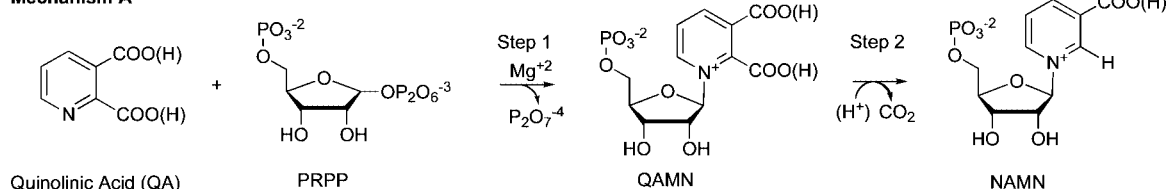
(13) Begley, T.; Kinsland, C.; Mehl, R.; Osterman, A.; Dorrestein, P. *Vitam. Horm.* **2001**, *61*, 103–119.

SCHEME 1

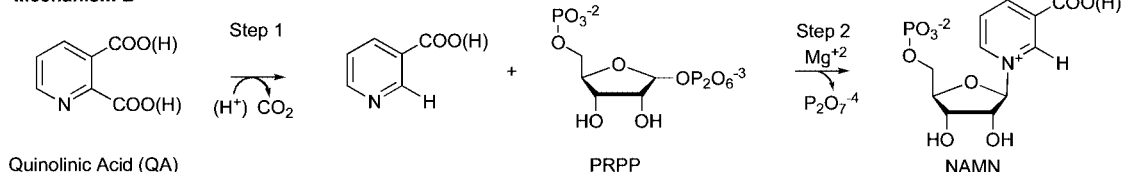


SCHEME 2

Mechanism A



Mechanism B



linic acid in cerebrospinal fluid.^{18,19} On the agricultural side, data suggest that QPRTase may play a role in the signal pathway for promotion of plant growth and protection.^{20,21} Despite the significance of the enzyme, the mechanism of action remains unknown.¹

One particularly intriguing aspect of this transformation is that the decarboxylation results in an anion that has no pi system into which to delocalize; this unusual feature is similar to the reaction catalyzed by orotidine 5'-monophosphate (OMP) decarboxylase, which we have also studied and which has been the subject of much recent study and debate.^{22–35} Such a

reaction is rare in biological decarboxylations, which typically form anions that are stabilized by delocalization.^{22–35} We were driven by our interest in these unusual decarboxylations to probe the QA to NAMN transformation. Our goal in this paper, as a first step, is to reveal the intrinsically most likely pathway for the transformation of QA and PRPP to NAMN.²³ Toward this end, we have calculated the reaction energetics of various models for possible substrates of QPRTase, both in the gas phase and in a water dielectric.

Results and Discussion

Mechanistic Possibilities. Although we are ultimately interested in the decarboxylation step, we need to consider *what substrate decarboxylates*. There are two prevalent mechanistic proposals for the overall transformation of quinolinic acid to NAMN: phosphoribosyl (PRPP) transfer *before* decarboxylation (Mechanism A, Scheme 2) and phosphoribosyl transfer *after* decarboxylation (Mechanism B, Scheme 2).^{2,36–40} Mechanism A involves the intermediate quinolinic acid mononucleotide (QAMN), which is a subject of debate regarding whether it is an intermediate in the enzyme-catalyzed reaction.^{2,36,37} We will first discuss the energetics associated with the phosphoribosyl transfer step in Mechanisms A and B, respectively.

(14) Balganes, T. S.; Balasubramanian, V.; Kumar, S. A. *Curr. Sci.* **2004**, *86*, 167–176.

(15) Zhang, Y.; Amzel, M. L. *Curr. Drug Targets* **2002**, *3*, 131–154.

(16) Duncan, K. *Curr. Pharm. Des.* **2004**, *10*, 3185–3194.

(17) Gerdes, S. Y.; et al. *J. Bacteriol.* **2002**, *184*, 4555–4572.

(18) Stone, T. W.; Perkins, M. N. *Eur. J. Pharmacol.* **1981**, *72*, 411–412.

(19) Heyes, M. P.; Saito, K.; Crowley, J. S.; David, L. E.; Demitrack, M. A.; Der, M.; Dilling, L. A.; Elia, J.; Kruesi, M. J.; Lackner, A. *Brain* **1992**, *115*, 1249–1273.

(20) Sinclair, S. J.; Murphy, K. J.; Birch, C. D.; Hamill, J. D. *Plant Mol. Biol.* **2000**, *44*, 603–617.

(21) Wang, K.; Conn, K.; Lazarovits, G. *Appl. Environ. Microbiol.* **2006**, *72*, 760–768.

(22) Begley, T. P.; Ealick, S. E. *Curr. Opin. Chem. Biol.* **2004**, *8*, 508–515.

(23) Lee, J. K.; Tantillo, D. J. *Adv. Phys. Org. Chem.* **2003**, *38*, 183–218.

(24) Callahan, B. P.; Miller, B. G. *Bioorg. Chem.* **2007**, *35*, 465–469, and references therein.

(25) *Orotidine Monophosphate Decarboxylase: A Mechanistic Dialogue*; Topics in Current Chemistry; Lee, J. K., Tantillo, D. J., Eds. Springer: Berlin, 2004; Vol. 238, and references therein.

(26) Miller, B. G.; Wolfenden, R. *Annu. Rev. Biochem.* **2002**, *71*, 847–885, and references therein.

(27) Radzicka, A.; Wolfenden, R. *Science* **1995**, *267*, 90–93, and references therein.

(28) Lee, J. K.; Houk, K. N. *Science* **1997**, *276*, 942–945.

(29) Kurinovich, M. A.; Phillips, L. M.; Sharma, S.; Lee, J. K. *Chem. Commun.* **2002**, 2354–2355.

(30) Wepukhulu, W. O.; Smiley, V. L.; Vemulapalli, B.; Smiley, J. A.; Phillips, L. M.; Lee, J. K. *Org. Biomol. Chem.* **2008**, in press.

(31) Singleton, D. A.; Merrigan, S. R.; Kim, B. J.; Beak, P.; Phillips, L. M.; Lee, J. K. *J. Am. Chem. Soc.* **2000**, *122*, 3296–3300.

(32) Phillips, L.; Lee, J. K. *J. Org. Chem.* **2005**, *70*, 1211–1221.

(33) Phillips, L.; Lee, J. K. *J. Am. Chem. Soc.* **2001**, *123*, 12067–12073.

(34) Raugi, S.; Cascella, M.; Carloni, P. *J. Am. Chem. Soc.* **2004**, *126*, 15730–15737.

(35) Warshel, A.; Strajbl, M.; Villa, J.; Florian, J. *Biochemistry* **2000**, *39*, 14728–14738.

(36) To our knowledge, Mg^{2+} has never been found in any crystal structure and its exact role is unknown. It has been proposed to help pyrophosphate depart,² or aid in the stabilization of the 5'-phosphate.³⁹ Because its exact role is unknown, and because we assume that its role would be the same in either mechanism (thus, "canceling" out when relative energetics are compared), we did not include Mg^{2+} in our calculations.

(37) Eads, J. C.; Ozturk, D.; Wexler, T. B.; Grubmeyer, C.; Sacchetti, J. C. *Structure* **1997**, *5*, 47–58.

(38) Liu, H.; Woznica, K.; Catton, G.; Crawford, A.; Botting, N.; Naismith, J. H. *J. Mol. Biol.* **2007**, *373*, 755–763, and references therein.

(39) Sharma, V.; Grubmeyer, C.; Sacchetti, J. *Structure* **1998**, *6*, 1587–1599, and references therein.

(40) Another mechanistic possibility is the protonation of QA at N1, which would induce C2 decarboxylation. Proton transfer from N1 to C2 would be followed by alkylation. We did not explore this path as it is not suggested in the biochemical literature, but it is a logical possibility.

SCHEME 3

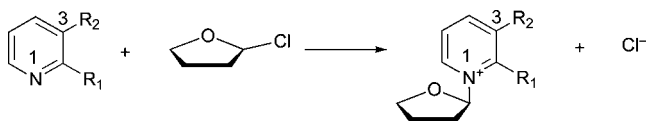


TABLE 1. ΔH (in kcal mol⁻¹) for Addition Reactions of 1–3 (Figure 1, Scheme 3; reactions are models for Step 1, Mechanism A, Scheme 2)^a

quinolinic acid derivative	addition of THF-Cl	
	(gas phase)	(water) ^b
1	122	3
2	26	-6
3	-63	-10
2cx	100	-
3cx	14	-

^a Calculated at B3LYP/6-31+G*. ^b Optimized at B3LYP/6-31+G* using the CPCM solvent model.

When considering the phosphoribosyl transfer, the immediate question is whether the reaction proceeds via S_N1 or S_N2.^{2,38,39,41} Unfortunately, this is unknown for QPRTase.^{2,38,39,41} Other PRTases proceed via inversion of stereochemistry at the anomeric ribose C1, implying S_N2.^{2,38,39,41-46} In light of the stereochemical data for other PRTases, we decided to focus on an S_N2-type mechanism for the addition, probing what substrates would be energetically favorable for such an addition.

Phosphoribosyl Transfer, Mechanism A. For Mechanism A (Scheme 2), we determined what form of quinolinic acid—the neutral (**1**), the 2-carboxylate anion (**2a**), the 3-carboxylate anion (**2b**), or the dicarboxylate dianion (**3**)—would result in the most energetically favorable PRPP transfer reaction. To model the PRPP transfer, we calculated the energetics associated with the reaction of **1–3** with 2-chloro-tetrahydrofuran (Scheme 3).^{36,39,41,44,47}

The energetics (ΔH) for the gas phase addition step are shown in Table 1.⁴⁸ The reaction of the neutral quinolinic acid **1** with THF-Cl is quite endothermic (122 kcal mol⁻¹ at B3LYP/6-31+G*). The monoanionic species **2a** and **2b**, when optimized, resolve to one structure, where the proton is shared between the two carboxylates (**2**, Figure 1); similarly, the product of the addition has the proton bridged between the two carboxylates.⁴⁹ This addition reaction is more favorable than that of **1**, with a ΔH_{rxn} of 26 kcal mol⁻¹. Not surprisingly, the most favorable reaction is that of the dicarboxylate **3**; this dianionic species reacts with THF-Cl exothermically, with a ΔH_{rxn} of -63 kcal mol⁻¹. We also calculated the energetics at MP2/6-31+G*/B3LYP/6-31+G* as a “check” and find consistent results (data in Supporting Information).

(41) Tao, W.; Grubmeyer, C.; Blanchard, J. S. *Biochemistry* **1996**, *35*, 14–21, and references therein.

(42) Chelsky, D.; Parsons, S. J. *Biol. Chem.* **1975**, *250*, 5669.

(43) Victor, J.; Greenberg, L. B.; Sloan, D. L. *J. Biol. Chem.* **1979**, *254*, 2647.

(44) Goitein, R. K.; Chelsky, D.; Parsons, S. M. *J. Biol. Chem.* **1977**, *253*, 2963–2971.

(45) Focia, P. J.; Craig III, S. P.; Eakin, A. E. *Biochemistry* **1998**, *37*, 17120–17127.

(46) For orotate phosphoribosyl transferase, although inversion of stereochemistry is observed, kinetic isotope effects do imply a transition state with much oxycarbonium character.⁴¹

(47) Begley, T. P.; Appleby, T. C.; Ealick, S. E. *Curr. Opin. Struct. Biol.* **2000**, *10*, 711–718.

(48) Hammond, G. S. *J. Am. Chem. Soc.* **1955**, *77*, 334–338.

(49) Perrin, C. L.; Nielson, J. B. *Annu. Rev. Phys. Chem.* **1997**, *48*, 511–544, and references therein.

We also wanted to ascertain whether these trends change in a polar solvent; the reactions in a water dielectric are also listed in Table 1. The values are not as large and are more realistic; the trend holds that dianion **3** shows the most favorable reaction, followed by monoanion **2** then neutral **1**, but the “spread” is not so drastic.^{49,50}

Because the crystal structure of QPRTase indicates stabilization of the carboxylates with ammonium groups (arginine and lysine), we also calculated a model with an ammonium ion (NH₄⁺) hydrogen bound to the monocarboxylate (**2cx**) and dicarboxylate (**3cx**) ions.⁵⁰ The monocarboxylate–ammonium complex has a ΔH_{rxn} of 100 kcal mol⁻¹, which is slightly better than the completely neutral **1** but still worse than the bare monocarboxylate **2**. Likewise, the ΔH_{rxn} for the dicarboxylate–ammonium complex **3cx** is not quite as favorable as the bare dicarboxylate **3** but is still more favorable than the formal monocarboxylate **2**.

Phosphoribosyl Transfer, Mechanism B. To probe the PRPP transfer in Step 2, Mechanism B (Scheme 2), where decarboxylation precedes addition, we determined the reaction energetics for the addition of decarboxylated derivatives of quinolinic acid (**4**, **5** Figure 2) plus THF-Cl.

The addition reaction of the monocarboxylate anion **4** is endothermic by 23 kcal mol⁻¹; that of **5** is even more endothermic (102 kcal mol⁻¹), presumably since it is neutral. This trend holds true as well at the MP2/6-31+G*/B3LYP/6-31+G* level (data in Supporting Information). In a water dielectric, both reactions have an exothermic ΔH_{rxn} , with **4** being more exothermic. The ΔH_{rxn} values in water also differ by only 3 kcal mol⁻¹ since the solvation mitigates the carboxylate charge effect of **4**.

We also calculated the ΔH_{rxn} in the gas phase for the complex of **4** and an ammonium ion, again to model the enzymatic reaction (**4cx**). The reaction is endothermic by 93 kcal mol⁻¹, making it more favorable than that of the neutral species **5** but not as favorable as that of the anion **4**.

Thus, for Step 2 of Mechanism B (Scheme 2, decarboxylation precedes addition), not surprisingly, structures with more anionic charge exhibit less endothermic/more exothermic enthalpies of reaction.

In considering Tables 1 and 2 together, it appears that in the gas phase, **2**, **3**, **3cx**, and **4** all have reasonable ΔH_{rxn} values for the addition reaction, with **3** being the most favorable. Water decreases the spread of ΔH_{rxn} values greatly; all the substrates **1–5** have favorable (exothermic or just slightly endothermic) ΔH_{rxn} values, with **4** being the most favorable.⁵¹ Of course, the values might change with the actual PRPP substrate, but these calculations show that the reaction enthalpies, particularly in water and also for the complex **3cx**, are within a reasonable range. We thus moved on to our main interest, the decarboxylation step.

Decarboxylation. Our goal was to probe the ease of decarboxylation for the various possible substrates. The next question to answer is what species decarboxylates most readily. We focused on the substrates in Figure 3, corresponding to decarboxylation before and after addition (Table 3).⁵² For all

(50) To properly consider solvation and enzyme site binding, specific interactions need to be considered; computationally this would involve QM/MM calculations, which would be the topic of a future study. For discussion on QM/MM methods see: Warshel, A. *Computer Modeling of Chemical Reactions in Enzymes and Solutions*; John Wiley and Sons: New York, 1991.

(51) We did not calculate the carboxylate–ammonium complexes in water since the complex itself is already hydrogen-bound and is designed to very roughly mimic the enzyme active site.

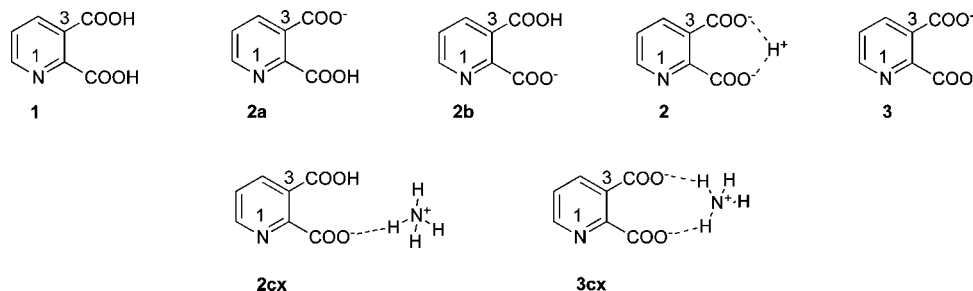


FIGURE 1. Possible quinolinic acid substrates (pre-decarboxylation).

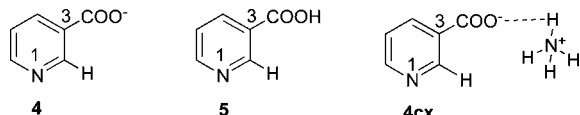


FIGURE 2. Possible quinolinic acid substrates (post-decarboxylation).

TABLE 2. ΔH (in kcal mol⁻¹) for Addition Reactions of 4–5 (Figure 2, Scheme 3; Reactions Are Models for Step 2, Mechanism B, Scheme 2)^a

quinolinic acid derivative	addition of THF-Cl	
	(gas phase)	(water) ^b
4	23	-15
5	102	-12
4cx	93	-

^a Calculated at B3LYP/6-31+G*. ^b Optimized at B3LYP/6-31+G* using the CPCM solvent model.

the reactions in Table 3, the listed values correspond to decarboxylation resulting in the anion at C2. We are assuming for now that the decarboxylation is a rate-determining step and that the decarboxylation product (the vinylic anion at C2) will undergo fast proton transfer for either mechanism in a step that is not rate-determining.^{25,28–33} We make this assumption because we are interested in comparing the ease of decarboxylation for each mechanism.

Decarboxylation of **2**, **3**, **2cx**, and **3cx** corresponds to decarboxylation preceding addition (Mechanism B, Scheme 2), while decarboxylation of **6**, **7**, **6cx**, and **7cx** corresponds to addition preceding decarboxylation (Mechanism A, Scheme 2).

In the gas phase, the more favorable decarboxylations involve species **6**, **7**, **6cx**, and **7cx**, which arise when addition is the first step (Mechanism A, Scheme 2).^{48,53} All the species after addition have an enthalpy of decarboxylation ranging from 11–29 kcal mol⁻¹ (Table 3, second column). In contrast, the decarboxylation of species **2**, **3**, **2cx**, and **3cx** (pertinent to Mechanism B, Scheme 2, decarboxylation preceding addition) is highly unfavorable, with enthalpies greater than 55 kcal mol⁻¹ in the gas phase (Table 3, second column). Thus, the decarboxylation reaction of the QAMN analogs **6**, **7**, **6cx**, and **7cx** is markedly more favorable than the decarboxylation of the quinolinic acid species **2**, **3**, **2cx**, and **3cx**. We also calculated the decarboxylation (at C2, the biologically relevant reaction) for **2**, **3**, **6**, and **7** in a water dielectric to assess the bulk effect

of a polar solvent on the reactions.⁵¹ We find that the same trend holds: the decarboxylation of **6** and **7** is more favorable than that of **2** and **3**. Interestingly, as an aside, the water dielectric actually increases the enthalpy of decarboxylation of **6** and **7** relative to the gas phase. Probably the stabilization in the zwitterionic products (C2 carbanion stabilization by the positively charged N1) is mitigated by the solvent dielectric.

Another interesting feature of the decarboxylation reaction is that the zwitterion **6** decarboxylates more readily than **7**, by about 10 kcal mol⁻¹ (Table 3, second column (gas phase); fourth column (water)). Similarly, the complex **6cx** decarboxylates more readily than **7cx** by about the same 10 kcal mol⁻¹ (Table 3, second column). That is, the presence of the anionic 3-carboxylate moiety in **7** and **7cx** actually slows down the decarboxylation at C2, relative to **6** and **6cx**. Thus for C2 decarboxylation, a C2 monocarboxylate is the favored substrate. Our results on the effect of a proximal anionic carboxylate on the decarboxylation of a zwitterionic species have also been observed by Kass and co-workers, who did not study QPRTase, but conducted a series of elegant studies of gas phase zwitterionic dicarboxylate species.^{54,55}

Additionally, we were curious, mostly for general mechanistic reasons, as to whether decarboxylation at C2 or C3 is a more favorable reaction. We find that it is more favorable to decarboxylate **6** and **7** at the C2 (not the C3) position (Table 3, second and third columns for the gas phase and fourth and fifth columns for water). Therefore, both **6** and **7** prefer to decarboxylate at the position that would lead to the desired NAMN product. This preference for C2 decarboxylation has also been observed by Kass and co-workers (who examined structure **7** where R=CH₃ (as opposed to THF) in the context of a series of dicarboxylate gas phase studies), who propose that the C2 site is favored due to the dipolar stabilization between N1 and C2 gained in the product.^{54–58}

In contrast, it is about 3–4 kcal mol⁻¹ easier to decarboxylate the C3 position of species **2** and **3** in the gas phase (Table 3, second and third columns), and 7–9 kcal mol⁻¹ easier to decarboxylate the C3 position of species **2** and **3** in water (Table 3, fourth and fifth columns). In the context of the QPRTase transformation, therefore, Mechanism B (Scheme 2) may be less attractive, due to the relative favorability of the biologically irrelevant C3 decarboxylation.

Thus, the most energetically favorable intrinsic path for decarboxylation is occurrence after addition (Mechanism A,

(52) The gas phase decarboxylations of **2**, **3**, **6**, and **7** were also calculated at MP2/6-31+G*/B3LYP/6-31+G*; values are consistent with the B3LYP/6-31+G* calculations (data in Supporting Information).

(53) Transition structures were found for **6**. All the other reactions are sufficiently endothermic that we see a monotonic increase in energy as the CO₂ departs; therefore, in these cases, the endothermicity reflects the activation enthalpy.⁴⁸

(54) Wang, X. B.; Dacres, J. E.; Yang, X.; Broadus, K. M.; Lis, L.; Wang, L.-S.; Kass, S. R. *J. Am. Chem. Soc.* **2003**, *125*, 296–304.

(55) Wang, X. B.; Dacres, J. E.; Yang, X.; Lis, L.; Bedell, V. M.; Wang, L.-S.; Kass, S. R. *J. Am. Chem. Soc.* **2003**, *125*, 6814–6826.

(56) Beak, P.; Siegel, B. *J. Am. Chem. Soc.* **1976**, *98*, 3601–3606.

(57) Dunn, E.; Thimm, F. *Can. J. Chem.* **1977**, *55*, 1342–1347.

(58) Dunn, G. E.; Lee, G. K. J.; Thimm, H. *Can. J. Chem.* **1972**, *50*, 3017–3027.

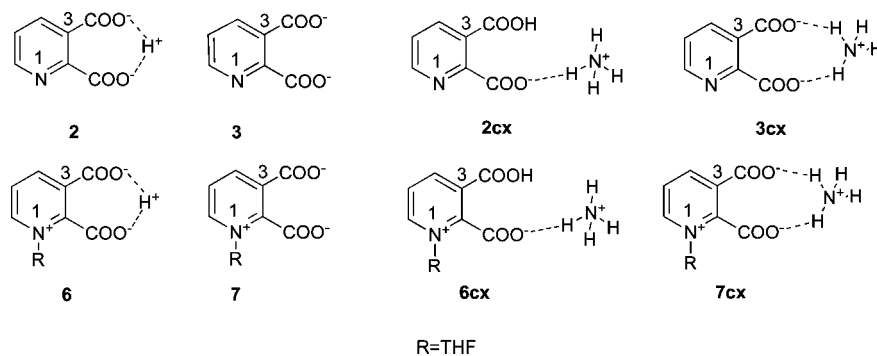


FIGURE 3. Possible substrates for decarboxylation.

TABLE 3. ΔH (in kcal mol⁻¹) for Decarboxylation Reactions^a

quinolinic acid derivative	decarboxylation at C2 (gas phase)	decarboxylation at C3 (gas phase)	decarboxylation at C2 (water) ^b	decarboxylation at C3 (water) ^b
2	63	60	56	47
3	64	60	58	51
2cx	58	—	—	—
3cx	71	—	—	—
6	11 [16] ^c	23	16 [21] ^d	37
7	25	34	27	41
6cx	18	—	—	—
7cx	29	—	—	—

^a Calculated at B3LYP/6-31+G*. ^b Optimized at B3LYP/6-31+G* using the CPCM solvent model. ^c Transition structure was found for the reaction of **6**; the ΔH^\ddagger value is in brackets. ^d The transition structure could not be found in a water dielectric (due to convergence issues); this is therefore a CPCM B3LYP/6-31+G* single point on the gas phase B3LYP/6-31+G* optimized transition structure.

Scheme 2), which allows for the more favorable decarboxylation of a species (QAMN) that is positively charged at N1.^{56,57} Decarboxylation through QAMN results in a reaction that is on the order of 30–50 kcal mol⁻¹ better (depending on medium).⁵⁹ Our calculations indicate that the best substrate for decarboxylation is structure **6** (and corresponding enzyme-model-ammonium complex **6cx**), which decarboxylates most favorably energetically and also favors decarboxylation at C2. Consequently, Mechanism A, Scheme 2 where addition precedes decarboxylation is the most energetically feasible pathway for the reaction. Both Mechanism A and Mechanism B will have the same overall ΔH , but Mechanism A avoids the prohibitively high barrier to decarboxylation that is likely in Mechanism B.

Overall Reaction and Comparison to Existing Experimental Data. We have shown that for our model system, the most attractive pathway for the transformation of QA to NAMN is Mechanism A (Scheme 2), where addition precedes decarboxylation. The substrate in the enzyme reaction is probably a mono- or dicarboxylate hydrogen bound to active site ammonium group(s).⁶⁰

Our calculations also indicate that QAMN, whose existence as an intermediate in the QPRTase reaction is under debate, is likely to be a player in the favored mechanism.^{2,37} The intermediacy of QAMN allows for a favorable decarboxylation. Furthermore, our calculations show which protonation states are favorable for each step. Zwitterion **6** will decarboxylate more readily than **7**, which may seem counterintuitive, but calculations reveal that a second carboxylate anion makes decarboxylation at C2 less favorable.^{54,55} Also not only do we find that zwitterion

6 decarboxylates more readily than monoanion **2** and dianion **3** but that **2** and **3** actually prefer decarboxylation at C3, which is completely at odds with the biological transformation.

With regard to our computational prediction in light of existing experimental data, the crystal structure of QPRTase has been determined for several different organisms, including *Salmonella typhimurium* (St-QPRTase; crystallized bound with QA and with NAMN), *Mycobacterium tuberculosis* (Mt-QPRTase; crystallized bound with QA, with NAMN, and with phthalic acid), *Helicobacter pylori* (Hp-QPRTase; crystallized bound with QA, with NAMN, with phthalic acid, and with 5'-phosphoribosyl-1'-(β -methylene) pyrophosphate), *Thermotoga maritima* (Tm-QPRTase; crystallized bound with NAMN), and *Homo sapiens* (h-QPRTase; crystallized bound with tartrate).^{36–39,61–63} The *M. tuberculosis* QPRTase structure suggests that the C2 carboxylate is present until the enzyme-catalyzed reaction is complete because lack of interaction between the negative C2 substituent with the positive Lys172 residue should facilitate release of NAMN from QPRTase.³⁹ These data thus support decarboxylation as the final step (Mechanism A, Scheme 2), since the C2 carboxylate appears to “hold” the substrate in the active site. If decarboxylation were to precede PRPP transfer (Mechanism B, Scheme 2, Step 1), the resultant substrate would not stay in the active site because there would be no C2-Lys interaction. Furthermore, our calculations indicate that quinolinic acid decarboxylates more favorably at C3, which is completely at odds with NAMN formation (*vide supra*).

(59) The decarboxylation of quinolinic acid has been studied in aqueous solution.⁵⁸ The N1-protonated, C2-carboxylate zwitterion appears to decarboxylate about twice as fast as the negatively charged C2-carboxylate anion. This is consistent with our studies showing that a positively charged N1 will enhance decarboxylation at C2.⁵⁶

(60) Jordan, F.; Li, H.; Brown, A. *Biochemistry* **1999**, *38*, 6369–6373.

(61) Kim, M. K.; Im, Y. J.; Lee, J. H.; Eom, S. H. *Proteins: Struct. Funct. Bioinf.* **2006**, *63*, 252–255.

(62) Kim, M. K.; Kim, Y. S.; Rho, S. H.; Im, Y. J.; Lee, J. H.; Kang, G. B.; Eom, S. H. *Acta Crystallogr.* **2003**, *59*, 1265–1266.

(63) Schwarzenbacher, R.; et al. *Proteins: Struct. Funct. Bioinf.* **2004**, *55*, 768–771.

In terms of substrate binding order, early kinetic experimental data implied that PRPP binding precedes QA binding.² However, several recent studies indicate that QA binding probably precedes PRPP binding.^{3,38,39} Furthermore, crystallographic studies show that the quinolinic acid binds deeper in the active site than PRPP, and that quinolinic acid binding leads to an enzyme conformational change that facilitates PRPP binding.^{38,39} Therefore, it appears that quinolinic acid binding precedes PRPP binding. The order of departure of the products from the active site is not as extensively studied; early work implies that pyrophosphate leaves the active site first, followed by carbon dioxide then by NAMN.^{2,3,38,39} Mechanism A is consistent with these experimental data, particularly the order in which the products are released, which is consistent with the order in which these products are generated in Mechanism A.

Conclusions

Our goal in this paper is to probe the decarboxylation associated with the quinolinic acid to nicotinic acid mononucleotide transformation. We discovered that the energetically favored mechanism involves: the addition of quinolinic acid to PRPP to yield the quinolinate monophosphate nucleotide intermediate (QAMN), followed by decarboxylation of the QAMN intermediate at the 2-position to ultimately yield the NAMN product. The QAMN intermediate is attractive because the positive charge at N1 renders decarboxylation at C2 more favorable (by 30–50 kcal mol⁻¹), presumably due to the dipolar stabilization between the positively charged N1 and the negatively charged C2 in the product.^{56,57} We also show that decarboxylation at C2 of QAMN is more favorable if the C3 carboxylate is as “neutral” as possible; that is, an anion at C3 actually slows down decarboxylation at C2. These studies represent the first step toward, ultimately, accurate QM/MM studies of QPRTase, a challenge for the future.^{34,35} The pathway we propose is also consistent with current existing experimental evidence, though more experiments will be necessary to test the specifics of our proposal.

Theoretical Methods

The geometries of all structures described were optimized using the B3LYP/6–31+G* method as implemented in Gaussian03.^{64,65} Frequency calculations were conducted as well. The B3LYP/6–31+G* method has been shown to yield reliable *relative* energetics for a wide variety of organic transformations, including decarboxylation reactions.^{28,31,33,66–68} We also conducted MP2/6–31+G* single point calculations on the B3LYP/6–31+G* optimized geometries where indicated.⁶⁹ Dielectric medium calculations were carried out using a conductor-like polarizable continuum solvent model (CPCM using UAKS radii, also at B3LYP/6–31+G*), as implemented in Gaussian03.^{64,70,71} For the decarboxylation calculations of the ammonium complexes, the bonds between the carboxylates and ammonium were frozen to prevent proton transfer to the product C2 vinylic anion. This was done in order to provide values that could be directly compared with the decarboxylations of the “naked” gas phase substrates.⁷²

Acknowledgment. We gratefully acknowledge the support of NSF, the Alfred P. Sloan Foundation, and the National Center for Supercomputer Applications. We also thank the reviewers for extremely helpful suggestions.

Supporting Information Available: Cartesian coordinates for all calculated species and full citations for references with greater than 16 authors. This material is available free of charge via the Internet at <http://pubs.acs.org>.

JO8012379

(64) Frisch, M. J. et al.; *GAUSSIAN 03, Rev. E.01*; Gaussian, Inc.: Wallingford CT, 2004.

(65) Kohn, W.; Becke, A. D.; Parr, R. G. *J. Phys. Chem.* **1996**, *100*, 12974.

(66) Bach, R. D.; Canepa, C. J. *J. Am. Chem. Soc.* **1997**, *119*, 11725–11733.

(67) Bach, R. D.; Canepa, C. J.; Glukhovtsev, M. N. *J. Am. Chem. Soc.* **1999**, *121*, 6542–6555.

(68) Li, J.; Brill, T. B. *J. Phys. Chem.* **2003**, *107*, 5993–5997.

(69) Hehre, W. J.; Radom, L.; Schleyer, P. v. R.; Pople, J. A. In *Ab Initio Molecular Orbital Theory*; Wiley: New York, 1986.

(70) Barone, V.; Cossi, M. *J. Phys. Chem.* **1998**, *102*, 1995–2001.

(71) Cossi, M.; Scalmani, N.; Rega, N.; Barone, V. *J. Comput. Chem.* **2003**, *24*, 669–681.

(72) The vinylic anion formed from decarboxylation is quite basic and proton transfer probably will occur quickly; it is also possible that the two steps will occur in concert.